Two-dimensional electron spin echo spectroscopy and slow motions[a)]

Glenn L. Millhauser and Jack H. Freed
Baker Laboratory of Chemistry, Cornell University, Ithaca, New York 14853

(Received 1 February 1984; accepted 16 March 1984)

A technique is described for the study of slow molecular motions that employs two-dimensional electron spin echo (2*D*-ESE) spectroscopy. An "echo-induced ESR spectrum" is obtained with a two pulse 90°$_{\mp}$180° sequence by recording the echo height as the dc field is swept. A series of sweeps with different τ are Fourier transformed to yield a two-dimensional spectrum comprised of an echo-induced spectrum along the x axis and the homogeneous widths along the y axis. A convenient theoretical analysis appropriate for slow motions is given and it is shown that the 2*D* spectrum may be regarded as a graph of the widths vs the resonance positions of the individual "dynamics spin packets" that constitute the spectrum. An experimental study of the spin probe Tempone in 85% glycerol/H_2O solvent for slow motions (i.e., rotational correlational times of order 10^{-5}–10^{-6} s) shows variations in homogeneous widths (i.e., T_2^{-1}) over the spectrum. This is analyzed in terms of canonical models of rotational reorientation—Brownian, free, and jump diffusion, and it is found that the variations of T_2^{-1} across the spectrum show features similar to a Brownian model. A special normalized contour plot of the 2*D* spectra is introduced which clearly emphasizes the variation of T_2^{-1} across the spectrum. The enhanced information content of these 2*D* spectra is discussed, and it is shown how 2*D*-ESE spectroscopy is both an improvement on and a complement to cw techniques for studying motional dynamics. Experimental extensions and limitations are also discussed.

I. INTRODUCTION

In a recent analysis of electron spin echoes[1] we have shown its potential utility in the study of slow motions such as are commonly observed from nitroxide (and other) spin probes in viscous solvents or from spin labeled macromolecules.[2] In that work, the emphasis was on the measurement of T_M, the phase-memory time, as an indicator of the (slow) rate of rotational reorientation. The time evolution of the echo decay for slow motions was found to be, in general, a complex phenomenon with the potential of providing extensive information on the nature of the motional process. The simple study of T_M could not itself be expected to do full justice to the richness of available information. In this work, we introduce a two-dimensional electron spin echo technique that is specifically designed to elicit more extensive information from the echo experiment on motional dynamics in the realm of slow motions.

A particular advantage of the echo experiment over cw techniques is that the time scale of this experiment T_M is essentially just the inverse of the homogeneous linewidth, which we will, for the present, simply call T_2, and this can be much longer than T_2^*, the inverse of the inhomogeneous line width, which affects the cw spectrum or equivalently the free-induction decay. It is this homogeneous T_2 that is sensitive to the motions. Thus, slower motions can be detected by echo methods.

We have shown that, in an ideal two pulse electron spin-echo experiment, the decay envelope is described by

$$S(\tau) = \mathrm{Re} \sum_{i,j} a_{ij} e^{(\Lambda_i + \Lambda_j^*)\tau}, \tag{1}$$

which is the real part of a sum of complex exponential functions.[1] The relevant parameters are determined by solving the stochastic Liouville equation which simultaneously includes the reversible quantum-mechanical spin dynamics and the irreversible molecular dynamics (treated classically). The Λ_j are the eigenvalues of the stochastic Liouville operator in the rotating frame. Their imaginary parts (i.e., Im Λ_j) represent the resonance frequencies of the associated "spin packets," while the real parts (i.e., Re Λ_j) represent their natural or homogeneous widths and are associated with the observed T_M (or T_2). The relative contribution of the various spin packets depends upon the coefficients a_{ij}, which are determined by the eigenvectors of the stochastic Liouville operator, the transition moments associated with the radiation field, and the magnitude of that field. [In Eq. (1) there is the possibility for beat terms between different spin packets when $i \neq j$ which can complicate the relation between the a_{ij} and the amplitudes of the spin packets.] One finds from the simulations that nitroxide slow-motional cw spectrum will typically consist of 50–200 such spin packets which make significant contributions. These spin packets overlap with one another (especially when the inhomogeneous width is included), and the typical broad envelope, i.e., the cw spectrum, is observed. Nevertheless, different spin packets contribute to different portions of the spectrum. Thus, if the Re Λ_j are different in magnitude from one another, one may expect to observe a T_2 that varies across the spectrum. The two-dimensional ESE technique that we describe is specifically designed to study variations of the natural width across the spectrum.

We are able to show in this study that such variations of natural T_2 across the spectrum are indeed expected on theoretical grounds and observed experimentally. One finds that in the rigid limit, T_2 is uniform over the sample. Since our 2*D*

[a)] Supported by NSF Grant No. CHE 8024124, NIH Grant No. GM-25862 and by the Cornell Materials Science Center (NSF).

 0021-9606/84/130037-12$02.10

ESE method is more sensitive to motions than is the cw spectrum, we mean by rigid limit in the present work that T_2 is dominated by solid-state intermolecular relaxation processes (e.g., spectral diffusion). However, even in the absence of such solid-state relaxation processes, it is possible for motions that are slow enough to have T_2 uniform over the sample according to our theoretical predictions. In the slow motional regime, however, the rotational motion does give rise to a variation of T_2 across the spectrum. Both the magnitude of T_2 and the way in which T_2 changes across the spectrum are found to be very dependent upon the character of the molecular motion responsible for the spin relaxation.

An ideal experiment to map these effects is a two-dimensional one. In the present work, we have taken a simple approach to achieve this. In our experiment we utilize a standard 90°$_\tau$180° two-pulse echo sequence and monitor the echo height at 2τ while slowly sweeping through the ESR spectrum by sweeping the dc magnetic field. This generates an "echo-induced ESR spectrum" for each value of τ. The resonant microwave field H_1 is kept small enough that it does not introduce any distortion into the echo-induced field-swept ESR spectrum (i.e., $|\gamma_e H_1| \ll \Delta\omega_s$, where $\Delta\omega_s$ is a measure of the width of spectral detail in the cw spectrum). After collecting a family of such spectra, a Fourier transform with respect to τ is performed at each field value. The resulting $2D$ spectrum yields the inhomogeneously broadened absorption-like echo-induced ESR spectrum in one dimension and the homogeneous line shape in the other dimension.

If we compare our approach with conventional approaches commonly utilized in $2D$-NMR[3] (in particular homonuclear J spectroscopy), one notes that in the latter it is preferred to use an H_1 large enough to irradiate the whole spectrum, so it is not necessary to sweep through the spectrum. Instead, at time 2τ, when the echo refocuses, data collection of the resulting free precession signal begins and is indexed by the parameter t'. This is repeated for a range of τ values. The resulting two-dimensional signal $S(\tau,t')$ is Fourier transformed with respect to both time variables. We will show that our $2D$ ESE experiment is closely related to this full time domain experiment. Our experiment, however, circumvents two difficulties that one would encounter in trying to perform the full time domain ESE experiment. First is the relatively low magnitude of H_1 in ESE. For uniform excitation of the absorption spectrum, it is necessary to satisfy the condition $|H_1| > |H_s|$, where H_s is the full width of the spectrum. H_1 typically cannot be made larger than 10–15 G in a pulse spectrometer operating with a low Q cavity (the low Q is necessary for rapid dissipation of the microwave pulse energy which must occur before signal detection), whereas it is common to measure ESR spectra that are 100 G (or more) wide. Hence the condition stated above is rarely met. The second difficulty arises from the limited bandwidth of modern transient recorders. State of the art instruments can digitize a waveform at a rate of 100 MHz (10 ns spacing) which corresponds to an ESR half-band spectral width of less than 18 G (the Nyquist limit). Techniques other than averaging transients can be implemented to increase the effective bandwidth, but this is done at the expense of increased data collection time. (In particular one can employ boxcar averaging along with 1 ns delay generators for a band width of 1 GHz, but a resonant microwave cavity with a $Q \sim 100$ at 9.3 GHz would act as a filter with a half-bandwidth of ~ 100 MHz).

The greater spectral detail we achieve in the $2D$-ESE map presents a new challenge to the study of the model dependence of rotational motions in the very slow motional regime. We are able to deal with the problem of accurate simulations of the $2D$ map by the use of our newer methods for rapidly and compactly diagonalizing the stochastic-Liouville operator.[4] Furthermore, we find that in the very slow motional regime, the analysis of Schwartz *et al.* for ESE[1] can be simplified.

In Sec. II we discuss the experimental procedures, the methods of data processing and results on the system of the spin-probe Tempone dissolved in glycerol/H_2O solvent. In Sec. III we discuss the method of spectral simulation, while in Sec. IV we compare experiment with theory. A summary and prospectus appear in Sec. V.

II. EXPERIMENTAL

A. Procedures

All experiments were carried out on the Cornell electron spin echo spectrometer. Synchronous control was established through an LSI 11/23 microcomputer which in turn operated through two interfaces, one to the 8080 microprocessor that drives the experiment and collects the data and another to a Varian gaussmeter. The field was scanned in a sawtooth fashion while being constantly monitored by the LSI which, at the appropriate field value, started the data collection. Each scan consisted of 500 data points, and there were typically 50–60 scans at different values of τ.

We display the results as the Fourier transform of τ. We have found that such displays are more convenient for representing the results and for highlighting the relevant aspects of the results. Thus, for example, the contour plots discussed below allow a direct estimation of T_2, its variation across the spectrum, and the actual spin-packet line shape (e.g., Lorentzian). Furthermore, in the Fourier transform, high frequency noise that exists in the data vs τ is eliminated, since we are only interested in the low frequency components of order T_2^{-1}.

Fourier transforms with respect to τ were handled in a standard manner by zero filling the arrays to 128 elements[5] (or 256 elements for the -65 °C spectrum), multiplying the resultant array by an apodization window of $\exp[-(t/b)^4]$ and applying the FFT algorithm. The value b was chosen so that no distortion of the contours assigned to slowly decaying regions of the spectrum was seen. This apodization scheme suppresses some of the experimental noise and allows for a smooth transition between the data array and its zero-filled addition. We display only the real part of the Fourier transform output (which has reflection symmetry about zero frequency) since this corresponds to the absorption spectrum. The spectrometer dead time τ_d (due mainly to cavity ringing) is 200 ns. To avoid introducing phase shifts upon Fourier transformation of the data we subtract the quantity τ_d from each value of τ so that the first data point is taken at $\tau = 0$. This is a legitimate practice as long as the τ

dependence of the observed signal is exponential. We have found from conventional spin echo experiments at various points across the spectrum that this is indeed the case.

In addition to zero filling and apodization we further enhanced the signal-to-noise ratio by Fourier filtering[6] each field scan (this was performed on the raw data, i.e., before final Fourier transformation into the field-frequency space). This step was especially necessary for distortion-free contour plots. An $\exp[-(t/a)^4]$ window was used where the width a was chosen so that no distortion was seen in the scans taken at short τ.

The sample chosen for study was Tempone in a 85% glycerol/water solution, which had been previously studied by cw[7] and ESE[8] methods. Preparation was handled in a manner previously described. The magnitude of H_1 was small enough that nuclear modulation due to Tempone or solvent protons was suppressed. The 90° pulse was 80 ns in duration, and this corresponds to an *effective* H_1 in the rotating frame of 1.1 G. (i.e., the effective H_1 is defined by $\gamma_e H_1 \tau_p \equiv \pi/2$).

Single field scans for short τ were checked to establish that: (1) the finite pulse magnitude did not cause artificial broadening of the spectra and (2) the boxcar time constant and spectrometer repetition rate were set so that no spectral distortions were introduced.

B. Results

Fully processed (i.e., filtered and Fourier transformed) two-dimensional spectra from a two pulse sequence are shown in Figs. 1(a)–1(c) for Tempone at − 100, − 75, and − 65 °C, respectively. The x or Gauss axis shows what is essentially the inhomogeneously broadened "echo-induced ESR signal," while along the y or width axis one finds the homogeneous line shape given as a function of position in the spectrum. Previous work[8] has demonstrated that at − 100 °C and below the phase memory time T_M is roughly independent of temperature (presumably due to solid-state relaxation mechanisms), and hence is not suitable for analysis by our stochastic models. We also know from previous studies that above this temperature motional effects play a dominant role in T_2 relaxation.

Although the two-dimensional surfaces are aesthetically pleasing, they are not very useful in extracting line shape information. To remedy this situation we introduce the normalized contour plot. For every field value we take the slice in the width direction and normalize it so that the corresponding amplitude at 0 MHz is unity. Such a contour map thus reveals only the homogeneous line shape as a function of field location.

In Figs. 2(a)–2(c) we show normalized contour maps for the three temperatures. (Each successive contour line represents a 10% change relative to the normalized maximum. Contours corresponding to low amplitudes, such that signal to noise was poor, have been omitted.) We also provide the slice in the field direction at 0 MHz to show how the contours relate to the observed spectrum. At − 100 °C, the contour lines are nearly parallel indicating uniform T_2 relaxation rates across the spectrum. Since the cw line shape does not change below this temperature, the parallel lines are consistent with the observation that the rigid limit has been achieved. At − 75 °C we clearly see effects due to motion. The contour lines are closest together (long relaxation time) in regions of the spectrum that are from radicals oriented such that one of the principal axes of their magnetic tensor is parallel to the external dc magnetic field (as determined from rigid limit simulations), a feature we discuss below.

At − 65 °C the contours also show variations that are expected to be motional effects but the structure is not as clear as in the − 75 °C case. Part of the problem is reduced signal-to-noise ratio due to the shorter phase memory time, which now becomes comparable to the spectrometer dead time. It is not clear whether the uneven contours at the low

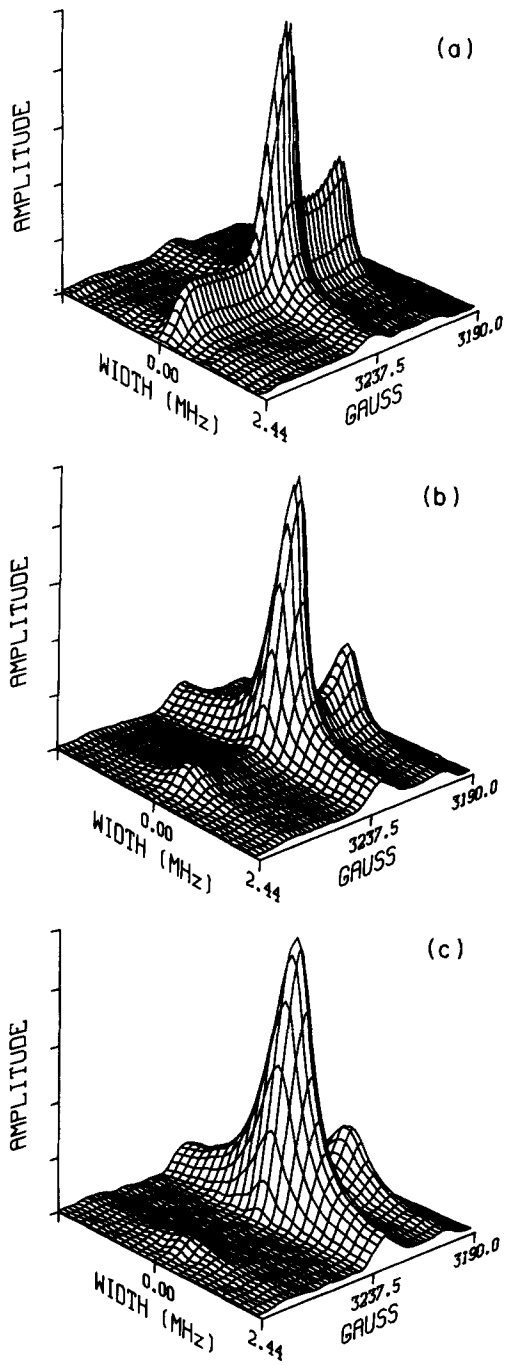

FIG. 1. The experimental two-dimensional spectra for Tempone in 85% glycerol/H_2O at (a) − 100 °C, (b) − 75 °C, and (c) − 65 °C.

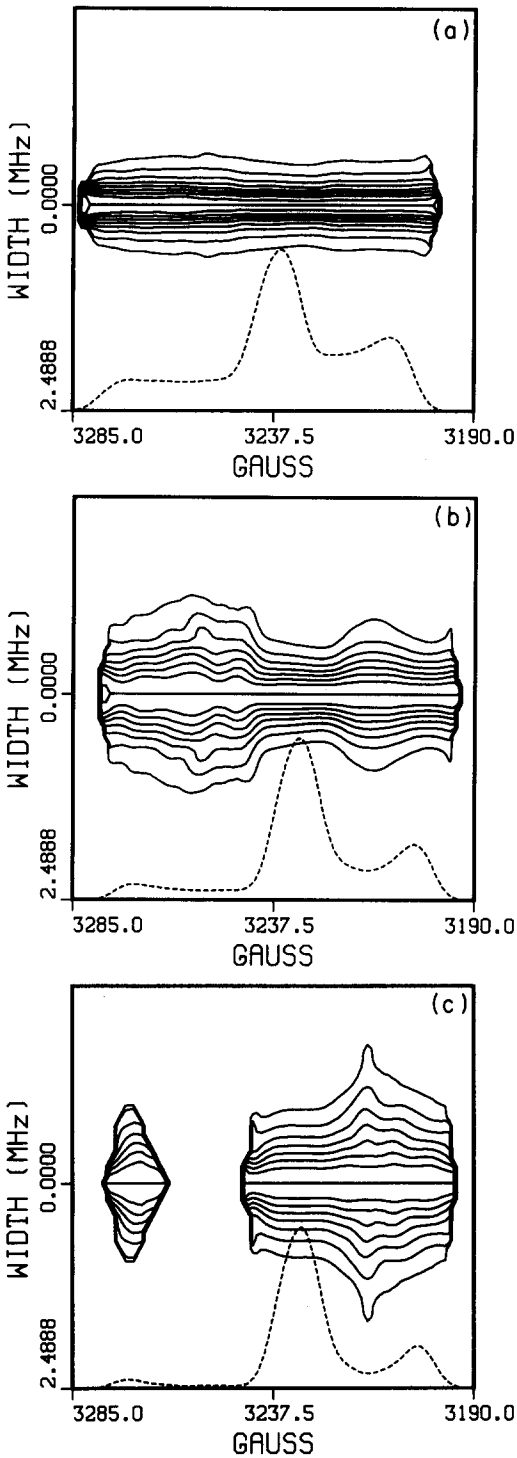

FIG. 2. The experimental normalized contours at (a) − 100 °C, (b) − 75 °C, and (c) − 65 °C. Each successive contour line represents a 10% change relative to the normalized maximum. Estimated T_2 values calculated from the width at 3235 G are 0.70, 0.44, and 0.28 μs, respectively. Shown at the bottom of each plot is the 0 MHz spectrum (see the text). In some plots we have deleted the low amplitude contours for clarity, since their signal to noise is low. [In particular, in Fig. 2(c) the spectral region from 3240–3260 G is too low in intensity to permit accurate contours.] Also, in this and the succeeding figures the vertical lines at each end closing the contours are artifacts of the plotting routines and should be ignored.

field amplitude minimum are due to motional effects (which are manifested as overlapping Lorentzian lines in the width direction) or simply noise, although results from our simulation studies indicate structure similar to what we observe (cf. below).

III. THEORY FOR SPECTRAL SIMULATIONS

To understand the two dimensional contours in a deeper manner and to provide a basis for simulation techniques we need to develop quantitative expressions for the echo-induced ESR experiment. We begin with the time-dependent form of the stochastic-Liouville equation[1] (SLE)

$$\dot{\hat{\rho}}(\Omega,t) = i[\hat{H}(\Omega),\hat{\rho}(\Omega,t)] - \Gamma_\Omega[\hat{\rho}(\Omega,t) - \hat{\rho}_0(\Omega)]. \quad (3)$$

Following the well known procedure of expanding the density matrix $\hat{\rho}(\Omega,t)$ in terms of eigenfunctions of the diffusion operator Γ_Ω and transforming into a rotating frame coordinate system,[1,9] we find the equation of motion for the vector of expansion coefficients to be

$$\dot{C}(t) = -\mathrm{B}\mathbf{C}(t). \quad (4)$$

B is a time-independent evolution operator derived from the stochastic-Liouville operator in the rotating frame. This equation holds for conditions of free precession, i.e., no radiation term in the Hamiltonian. Starting with the solution to Eq. (4) and the initial conditions as determined by the 90° pulse (designated by the vector **U**) gives

$$\mathbf{C}(\tau) = e^{-\mathrm{B}\tau}\mathbf{U}. \quad (5)$$

Applying the effects of the 180° pulse[1] and then allowing evolution for the time period $\tau + t'$ (where $t' > 0$), the total time evolution of the system is described by

$$C(2\tau + t') = e^{-\mathrm{B}(\tau+t')}e^{-\mathrm{B}^*\tau}\mathbf{U}^*. \quad (6)$$

The averaged signal is written as

$$S(2\tau + t') = \mathrm{Re}\{\mathbf{U}^{\mathrm{tr}}e^{-\mathrm{B}(\tau+t')}e^{-\mathrm{B}^*\tau}\mathbf{U}^*\}, \quad (7)$$

which, in matrix element notation, becomes

$$\begin{aligned} S(2\tau + t') &= \mathrm{Re}\sum_{ijklm} U_k O_{kl} O_{il} O^*_{ij} O^*_{mj} U^*_m \\ &\quad \cdot \exp[-(\Lambda_l + \Lambda^*_j)\tau]\exp[-\Lambda_l t'] \\ &\equiv \mathrm{Re}\sum_{lj} a_{lj}\exp[-(\Lambda_l \\ &\quad + \Lambda^*_j)\tau]\exp[-\Lambda_l t'], \end{aligned} \quad (8)$$

where O is the complex orthogonal matrix that diagonalizes B and Λ_l is the l th eigenvalue of B. If we set $t' = 0$ we recover the previously obtained result that the general decay envelope is a sum of complex exponential functions.[1] Thus, the eigenvalues of the stochastic Liouville operator are normal modes which make independent contributions to the ESR spectrum. We shall refer to each normal mode as a "dynamic spin packet" or just spin packet for short.

Near the rigid limit the elements of the complex orthogonal matrices O become nearly real.[1] Taking advantage of the properties of real orthogonal matrices we find

$$\begin{aligned} a_{lj} &\simeq \sum_{k,m} U_k O_{kl} O_{mj} U^*_m \sum_i O_{il} O_{ij} \\ &= \delta_{l,j}\sum_{k,m} U_k O_{kj} O_{mj} U^*_m. \end{aligned} \quad (9)$$

Thus, the only contributing terms to Eq. (8) are those where $l = j$. In general, **U** is purely imaginary.[1] Thus Eq. (9) can be written compactly as

$$a_{jj} = (\mathrm{O}^{\mathrm{tr}}\mathrm{U})_j^2 \tag{10}$$

and Eq. (9) becomes

$$S(2\tau + t') = \sum_j (\mathrm{O}^{\mathrm{tr}}U)_j^2 \exp[-2\,\mathrm{Re}\,\Lambda_j\tau] \times \exp[-\mathrm{Re}\,\Lambda_j t']\cos[\mathrm{Im}\,\Lambda_j t']. \tag{11}$$

Equation (11) shows explicitly that after a period 2τ the echo itself decays like a typical free induction decay with the exception that the amplitude of the jth term is now a function of τ and $\mathrm{Re}\,\Lambda_j$. Of course Eq. (11) does not describe the echo-induced ESR experiment since it is assumed in the derivation that $|H_1|$ is large enough to irradiate the whole spectrum whereas in our experiment $|H_1|$ is too small to accomplish this. In previous work[1] this feature was dealt with by restricting the summation in Eq. (11) only to those spin packets which are significantly affected by the radiation field. We now wish to improve on this approach. A somewhat relevant expression can be obtained if we recognize that the free induction decay in t' of the whole spectrum given by Eq. (11) would be just the Fourier transform of a spectrum[10] that is cw in ω' (and obtained with vanishingly small H_1) given by

$$S(2\tau,\omega') = \sum_j (\mathrm{O}^{\mathrm{tr}}\mathrm{U})_j^2 \exp[-2\,\mathrm{Re}\,\Lambda_j\tau] \times \frac{\mathrm{Re}\,\Lambda_j}{(\mathrm{Re}\,\Lambda_j)^2 + (\omega' - \mathrm{Im}\,\Lambda_j)^2}, \tag{12}$$

where $\omega' \equiv \gamma_e(H_0 - H_c)$; H_0 is the dc field value, while H_c is its value at the center of the spectrum (i.e., $\gamma H_c \equiv \omega_c$, the microwave frequency). If we now introduce inhomogeneous broadening by a Gaussian distribution of half-width Δ, then Eq. (12) becomes the convolution:

$$S(2\tau,\omega') \propto \sum_j (\mathrm{O}^{\mathrm{tr}}\mathrm{U})_j^2 \exp[-2\tau/T_{2,j}] \times \int_{-\infty}^{\infty} \exp[-(\omega' - \omega'')^2/\Delta^2] \times \frac{T_{2j}}{1 + (\omega'' - \omega_j)^2 T_{2,j}^2}\, d\omega'', \tag{13}$$

where we have let $\mathrm{Re}\,\Lambda_j = T_{2,j}^{-1}$ and $\mathrm{Im}\,\Lambda_j \equiv \omega_j$.

Although, in our experiment we sweep through H_0 very slowly, we are not actually performing a cw experiment. Furthermore, Eq. (12) implies a cw experiment wherein $|\gamma H_1| \ll T_{2,j}^{-1}$. Our *effective* H_1 of ~ 1.1 G would then translate into $T_{2,j} \ll 50$ ns by such an inequality. In actual fact, the $T_{2,j}$'s we obtain (cf. below) are *much longer* than 50 ns, so that we have $|\gamma H_1| \gg T_{2,j}^{-1}$. This latter inequality means that each spin packet at resonance will be uniformly rotated by the pulses. The experimental condition that $\gamma H_1 \ll \Delta\omega_s$, so as not to distort the "echo-induced ESR spectrum," thus still allows for effective rotation by the pulses as the packet is slowly swept into resonance. Instead, the experimental observation that an *effective* $H_1 \sim 1.1$ G is small enough not to introduce distortions is consistent with inhomogeneous broadening of $\Delta/\gamma \sim 3$–4 G that one observes for the Tempone sample in the near-rigid limit.[8,9b] Since $\Delta \gg T_{2,j}^{-1}$, it follows that the inhomogeneous broadening Δ will be the determining factor as to which spin packets are near enough to resonance to be effectively rotated by the pulses. Summarizing then, our experiment corresponds to the set of inequalities:

$$\gamma H_s > \Delta\omega_s \sim \Delta \gg \gamma H_1 \gg T_{2,j}^{-1}. \tag{14}$$

Thus, we may simply regard the definite integral in Eq. (13) as expressing the extent to which the inhomogeneously broadened spin packets are effectively rotated by the pulses and choose Δ accordingly. Furthermore, since $\Delta \gg T_{2,j}^{-1}$, the Lorentzian term acts as a delta function in the integrand, so we obtain:

$$S(2\tau,\omega') \propto \sum_j (\mathrm{O}^{\mathrm{tr}}\mathrm{U})_j^2 \exp[-2\tau/T_{2,j}] \times \exp[-(\omega' - \omega_j)^2/\Delta^2]. \tag{15}$$

Equation (15) is obtained from Eq. (13) for any shape function replacing the Lorentzian provided only it is much sharper than the inhomogeneous broadening, so that in this limit Eq. (15) is quite general.[11(a)] Thus, under the limiting conditions of Eq. (14), our experiment becomes virtually equivalent to the Fourier transform in t' of Eq. (11), which is then simply given by Eq. (15).[11(b)] Now a second Fourier transform (with respect to 2τ) yields the two-dimensional spectrum given by

$$S(\omega,\omega') \propto \sum_j (\mathrm{O}^{\mathrm{tr}}\mathrm{U})_j^2 \frac{T_{2,j}}{1 + \omega^2 T_{2,j}^2} \times [e^{-2\tau_d/T_{2,j}}]\exp[-(\omega' - \omega_j)^2/\Delta^2], \tag{16}$$

where we have included the effect of the finite deadtime τ_d. Note that for $\omega = 0$ we almost recover the expression for the cw line shape (with Gaussian inhomogeneous broadening) except for the effects of the deadtime and the extra factor of $T_{2,j}$ multiplying the amplitude of each spin packet.

Our simulations have been performed utilizing Eq. (16).

IV. DISCUSSION

A. Comparison between theory and experiment

The three canonical diffusion models used in our simulations are (1) Brownian diffusion, (2) jump diffusion in which a molecule has a fixed position for a time τ and then instantaneously reorients, and (3) approximate free diffusion in which a molecule rotates freely for a time τ and then instantaneously reorients.[9] Brownian motion is characterized solely by the diffusion constant R, whereas the other two models are characterized by both R and a residence time $\hat{\tau}$. The motional correlation time τ_R is expressed in terms of these parameters by the relation

$$\tau_R = (6B_2R)^{-1}, \tag{17}$$

where $B_2 = 1$ for Brownian motion, $B_2 = [1 + 6R\hat{\tau}]^{-1}$ for jump diffusion and $B_2 = [1 + 6R\hat{\tau}]^{-1/2}$ for approximate free diffusion. The product $R\hat{\tau}$ determines whether the process is of the strong jump type ($R\hat{\tau} > 1$), moderate jump type ($R\hat{\tau} \approx 1$) or weak jump type ($R\hat{\tau} < 1$).

In the work of Hwang, Mason, Hwang, and Freed (HMHF) Tempone in glycerol/water was studied by cw ESR in both the motionally narrowed regime and the slow motional regime.[7] An analysis of the motionally narrowed re-

sults showed that Tempone was reorienting isotropically. In the slow motional regime, where model dependence is distinguished, it was found that the most appropriate model was either moderate jump diffusion or approximate free diffusion (with $R\hat{\tau} \sim 1$).

To analyze our two-dimensional spectra we have studied three different diffusional models all taken to be isotropic: Brownian; jump ($R\hat{\tau} = 1$); and free diffusion ($R\hat{\tau} = 1$). We first considered whether the orthogonal matrices O had negligible imaginary components. In those cases utilized to simulate our experiments this criterion was easily satisfied for all of the eigenvalues contributing to the spectra, so that Eq. (16) was applicable. In our comparisons between theory and experiment was emphasized the shape and magnitude of the normalized contour plots across the spectrum (i.e., the T_2^{-1} across the spectrum). Only after reasonable satisfactory fits to the contours were obtained did we consider the line shape in the field direction, which necessarily includes substantial effects of inhomogeneous broadening. More specifically, the fitting criterion was to match the contour spacings in the low field region of the spectrum between 3200 and 3220 G. This spectral regime was found to be both well resolved experimentally and very sensitive to changes in the correlation times used in the simulations. (The intense central region of the spectrum yields contours that show a weaker dependence on changes in the correlation time; cf. Fig. 3.)

In Figs. 3(a)–3(d) we show simulations for the Brownian model and in Figs. 4(a)–4(d) we show simulations for the free diffusion model. The effects of the 200 ns dead time and 4 G inhomogeneous broadening are included. For a moderate jump model the normalized contours showed only parallel lines (i.e., no T_2 variation across the spectrum) for the full range of correlation times that give T_2 values consistent with those measured. This uniformity is not in agreement with our experimental findings, and we believe this tends to rule out such a model.

When we compare the normalized contour at -100 °C with the simulations [i.e., Figs. 2(a), 3(b), and 4(b)] we find no significant model dependence; both fit moderately well. The spectra generated from the 0 MHz cut of the unnormalized contours slightly favor the free diffusion model. At -75 °C [Figs. 2(b), 3(c), and 4(c)] the effects of motion are apparent. Both simulations show the characteristic diminished spacing between successive contour lines near the center of the spectra. In the free diffusion simulation, however, all other regions of the spectrum show parallel lines. The Brownian model shows another region of narrowing near the low field end of the spectrum around 3200 G which is more consistent

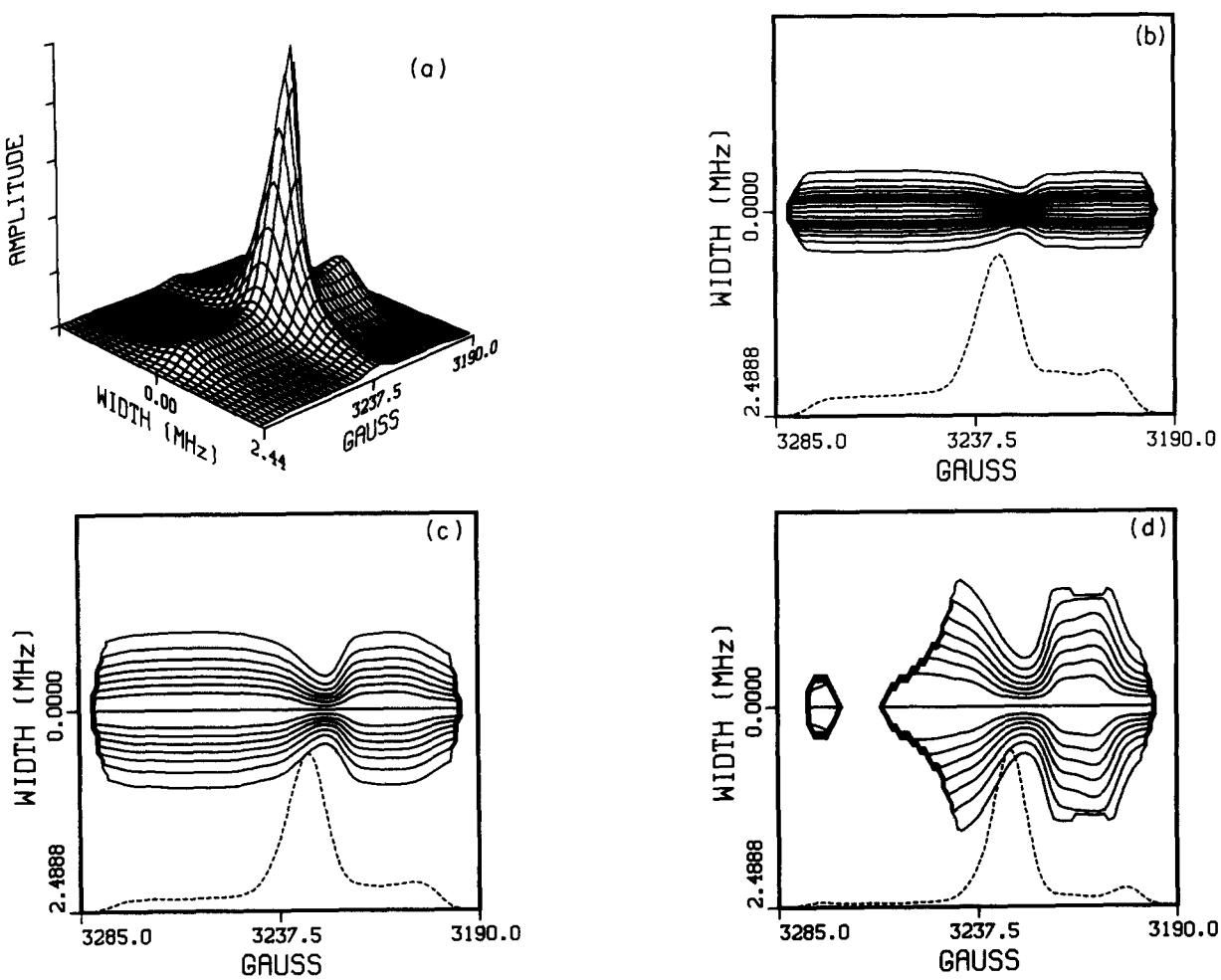

FIG. 3. Simulations of two-dimensional spectra utilizing a Brownian diffusion model. The effects of a 200 ns dead time and 4 G inhomogeneous broadening have been included. (a) Two-dimensional surface with $\tau_R = 3.33 \times 10^{-5}$ s, (b), (c), and (d) normalized contours with τ_R equal to 8.33×10^{-5} s, 3.33×10^{-5} s, and 1.67×10^{-5} s, respectively. In the plots the low amplitude contours deleted were chosen to match the experimental displays.

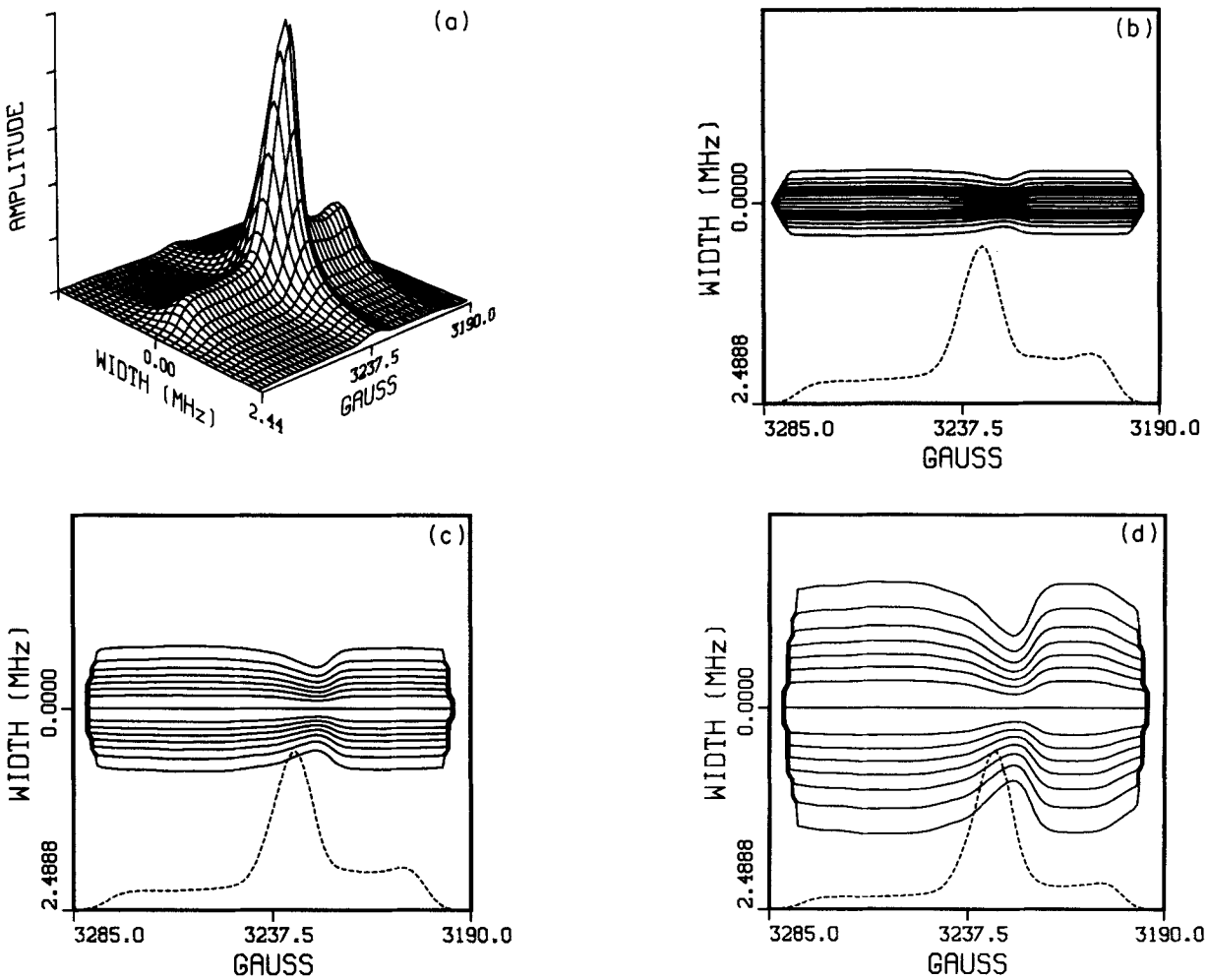

FIG. 4. Simulations of two dimensional spectra utilizing the model of approximate free diffusion. The effects of dead time and inhomogeneous broadening have been included as in Fig. 3. (a) Two-dimensional surface with $\tau_R = 3.53\times10^{-6}$ s; (b), (c), and (d) normalized contours with τ_R equal to 8.81×10^{-6} s, 3.53×10^{-6} s, 1.76×10^{-6} s. (See Fig. 3 for additional comments.)

with the experiment. Neither model shows the large contour variation seen in the high field region of the experimental spectrum between 3245 and 3275 G. The 0 MHz spectrum does not match very well for either model in the low field region between 3190 and 3220 G. (This was also true for the -100 °C set, for which the simulated spectra have converged practically to the rigid limit. This could imply the usual imperfections in fitting rigid limit spectra.[7,9])

At -65 °C [Figs. 2(c), 3(d), and 4(d)] the experimental $2D$ spectrum shows several details that are more prominent in the Brownian simulation. In the low field region between 3205 and 3220 G the contours are concave about the 0 MHz line. At the two ends of the 0 MHz spectrum the amplitudes rise before falling to zero out of the spectral range.

We find Brownian motion to be the somewhat more satisfactory model in the range of temperatures studied. This is in contrast with the previous work of HMHF but it should be noted that conventional cw spectra are not sensitive to changes in τ_R when this close to the rigid limit. Thus HMHF studied model dependence in the regime $\tau_R \sim 10^{-8}$ to 5×10^{-8} s, while in this work $\tau_R \sim 10^{-6} - 5\times10^{-5}$ s.

We have also explored the effects of anisotropy in the rotational diffusion[7,9] upon the predicted contours. Anisotropic rotational diffusion does, indeed, modify the appearance of the contours, but for small anisotropies (e.g., $N \equiv R_\parallel / R_\perp \approx 2$ where $R_\perp$ and $R_\parallel$ are the perpendicular and parallel components of the diffusion tensor) the same qualitative features remain.

To further demonstrate the potential usefulness of our experiment, we have generated simulations without the effects of dead time for τ_R's that are both shorter than what could now be experimentally probed and are near the limit of applicability of Eq. (16). We find the limiting τ_R values for Eq. (16) to be valid: 10^{-7} s for Brownian motion, 5×10^{-7} s for free diffusion and 5×10^{-8} for jump diffusion. In Figs. 5 and 6 we show normalized contours at short τ_R for the Brownian and free diffusion models, respectively. In general we find that the Brownian model yields greater variations in the contour shapes when one compares results corresponding to similar values of T_2. It should be noted that τ_R for the Brownian model is almost one order of magnitude longer than the corresponding value for free diffusion. In addition, there is a somewhat closer similarity of the 0 MHz unnormalized line shapes for the Brownian case vs the experimental result (in particular in showing amplitude minima at 3215 and 3260 G). Nevertheless, as noted above, the line shapes

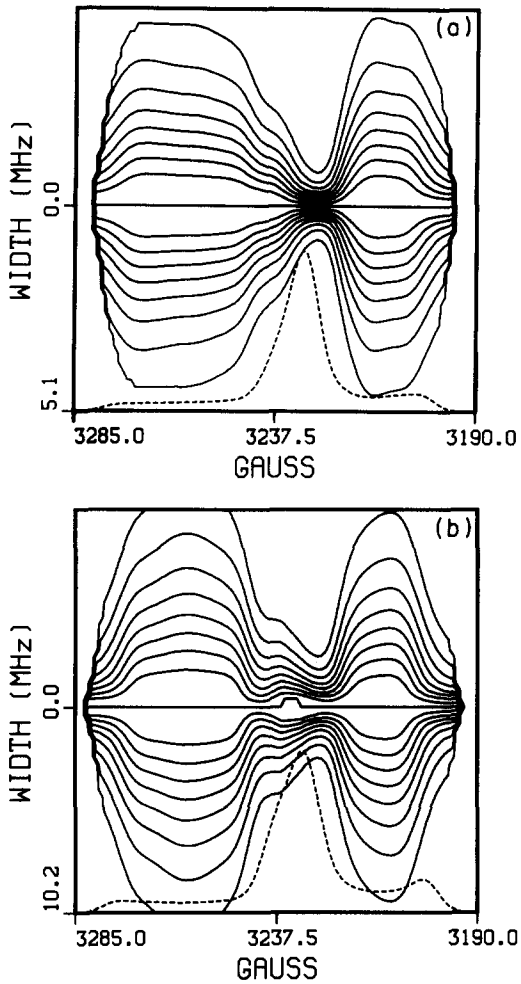

FIG. 5. Simulations of two-dimensional spectra for the Brownian diffusion model for shorter τ_R. Inhomogeneous broadening of 4 G has been included. The dead time has been set to zero. (a) $\tau_R = 8.33\times10^{-6}$ s, (b) $\tau_R = 4.17\times10^{-6}$ s. Note different scales along width axis.

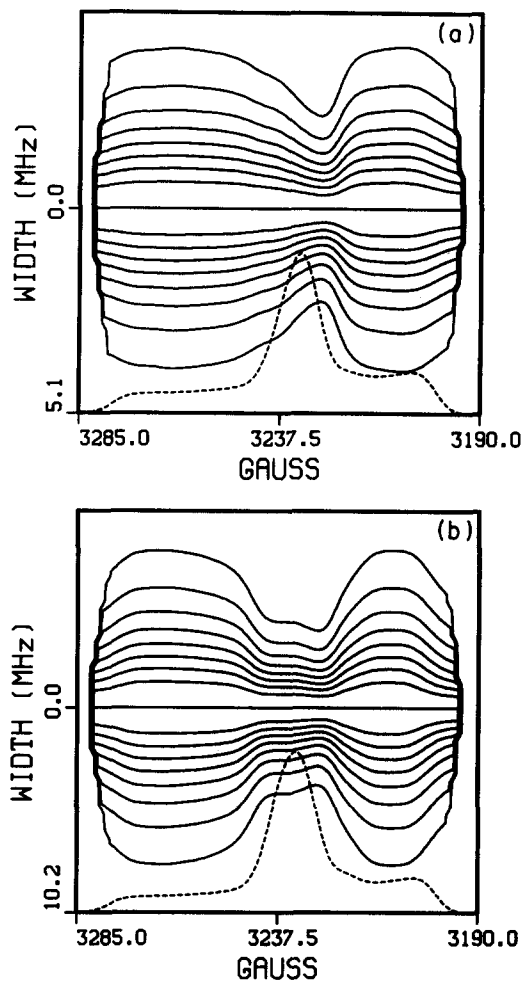

FIG. 6. Simulations of two-dimensional spectra for the model of Approximate Free Diffusion for shorter τ_R. (a) $\tau_R = 8.82\times10^{-7}$ s, (b) $\tau_R = 4.41\times10^{-7}$ s. See Fig. 5 for additional comments.

along the field direction do not show especially good agreement between theory and experiment even after we first choose the models to fit the contours.

In Fig. 7 we show a simulation for the jump model with $\tau_R = 2.33\times10^{-8}$ s which is considerably shorter than the τ_R's used to generate fits to experiment from the other models. It emphasizes that even in a regime of τ_R which should be very model sensitive (based upon observations of cw line shape changes), we still do not observe any variations in the shape of the contours from that of parallel lines.

To emphasize the profound effect of spectrometer dead time we show in Fig. 8 the same model used in Fig. 5(a) (i.e., for substantially faster τ_R then we studied) with the added effect of a 200 ns τ_d. The T_M calculated from contours at the center of this spectrum (where T_M is the longest) is $\sim$300 ns and hence easily measureable by conventional spin echo techniques. The dead time effect acts as a filter which evens the contours and removes much of the detail that allows one to distinguish among motional models. Examination of the 0 MHz unnormalized spectrum shows amplitudes in regions other than the center of the spectrum to be greatly reduced and explains why our two-dimensional approach becomes much more difficult to apply when τ_R, hence T_M, is this short.

In the work of HMHF it was found that τ_R obtained from the fast motional regime ($\tau_R \sim 10^{-10}$–10^{-9} s) followed

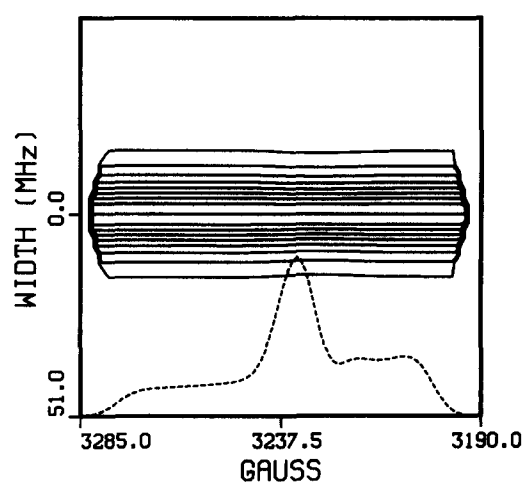

FIG. 7. Simulation of two-dimensional spectrum for the Jump diffusion model for shorter τ_R (2.33×10^{-8} s). See Fig. 5 for additional comments.

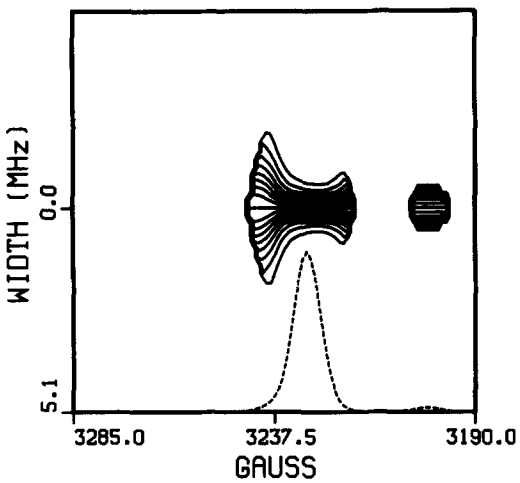

FIG. 8. Simulation of two-dimensional spectrum showing the effect of a 200 ns dead time. The motional model used in Brownian diffusion with $\tau_R = 8.33 \times 10^{-6}$ s [see Fig. 5(a)].

an Arrhenius plot with an activation energy $E_a = 15.2$ kcal/mol. We show in Fig. 9(a) the extrapolation of the Arrhenius fit of HMHF to the regime studied in the present work (i.e., 10^{-5}–10^{-6} s), and we also show the τ_R's obtained from simulating the $2D$ contours for the two models of Brownian and approximate free diffusion. In Fig. 9(b) we combine the present results on T_2 (or T_M) from the center of the spectrum with the more extensive previous measurements[1,8] of T_M, and one can see that they are in agreement, as they should be. The predictions of T_M for the different models are also shown. They are again based upon the extrapolated τ_R's from HMHF. For both ways of comparing experiment with theory [i.e., Figs. 9(a) and 9(b)], the agreement is surprisingly close considering that the Arrhenius plot was extrapolated almost five orders of magnitude in τ_R (e.g., E_a might have been expected to show some temperature dependence). In particular, the agreement of the Brownian model with the Arrhenius extrapolation is quite good and this is consistent with our analysis of the two-dimensional contours.

The apparent deviation of the -100 °C result from the Arrhenius plot is likely due to τ_R having become long enough that solid-state spectral diffusion processes are now making a significant contribution to T_M,[8] but the possibility of non-Arrhenius behavior at such high viscosities cannot be entirely ruled out.[12,13]

B. Further discussion

We comment further on the model dependence observed in this two-dimensional study and compare it with the

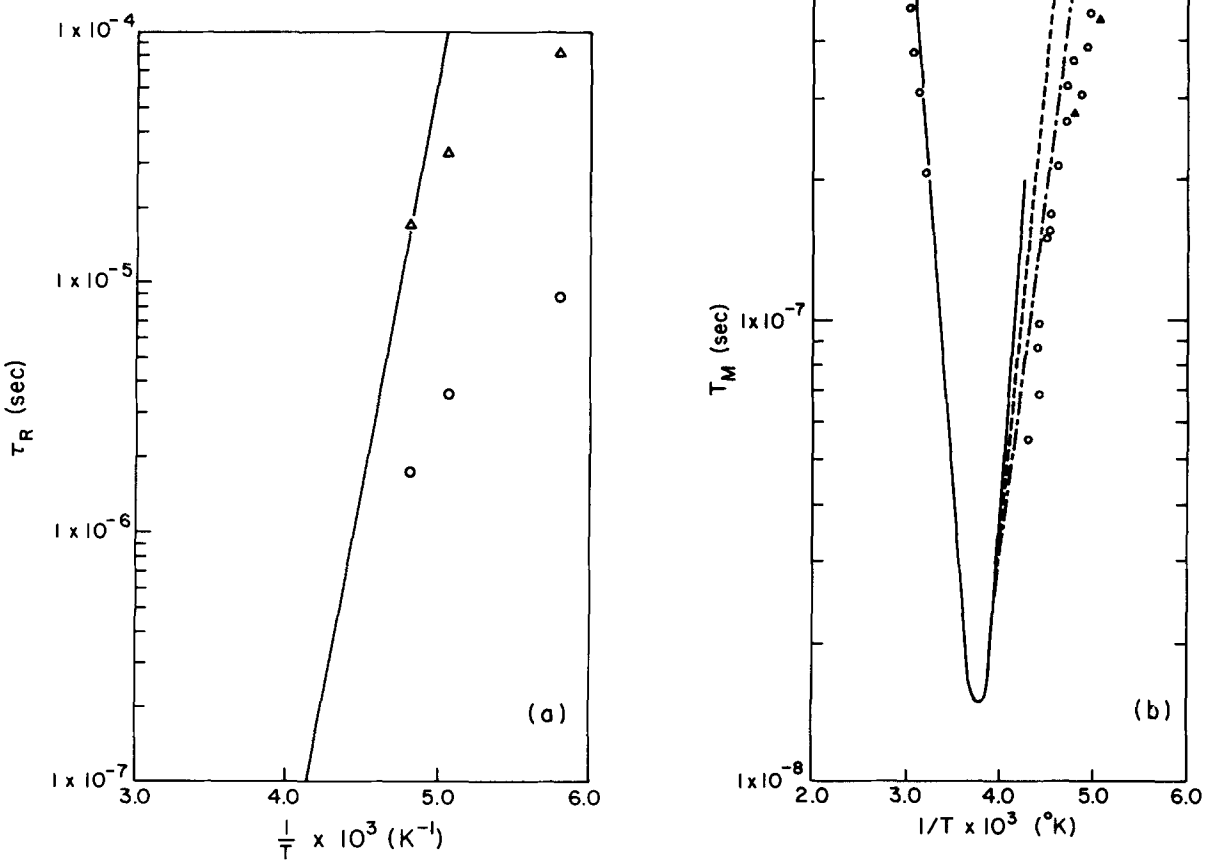

FIG. 9(a). Graph of τ_R vs T^{-1}. The solid line shows the τ_R extrapolated from the results of HMHF for the motionally narrowed regime. The triangles show the values of τ_R from the simulations based on Brownian diffusion (cf. Fig. 3) while the circles are from the simulations based on free diffusion (cf. Fig. 4). (b) Plot of T_M (or T_2) vs T^{-1}. The circles show T_M data from Schwartz *et al.* (Refs. 1 and 8). The triangles show the T_M from this study as measured from the contour plots at 3235 G. The different lines represent T_M in the central spectral regime calculated for the models of jump diffusion (solid line), free diffusion (dashed line), and Brownian diffusion (dashed–dotted line). The calculations employed the values of τ_R extrapolated from HMHF.

previous result of HMHF. First we note that the cw spectra, even in the model sensitive region, did not allow HMHF to distinguish between the canonical moderate jump vs free diffusion models. The two-dimensional contours are, however, unequivocal. Furthermore, these 2*D* results tend to favor Brownian motion somewhat over approximate free diffusion, but the experimental contours are somewhat flatter than predicted, as though the Brownian model would need some modification for small jumps.

In the regime of $\tau_R \sim 10^{-8}$ the cw results of HMHF clearly favored moderate jump over a Brownian model both in fitting the line shapes and in the Arrhenius extrapolations. We wish to comment on this apparent discrepancy from a point of view expressed in some detail by HMHF. Based upon their motional narrowing results they proposed a model in which they approximately included a finite relaxation time(s) τ_M for the fluctuating torques acting on the molecule. This corresponds to a memory effect which leads to a frequency dependent rotational diffusion coefficient given in lowest order as

$$R(\omega) \approx R(\omega = 0)[1 + i\omega\tau_M].^{14}$$

HMHF go on to note that in the slow motional theory, this will lead to some formal similarities compared to a jump model (e.g., one can define an *effective* relaxation time for the L^{th} spherical Harmonic that has a form identical to that from the jump model[7]), so they suggest that the "fluctuating torque" model might account for the observed cw line shapes. Stillman, Schwartz, and Freed[8] briefly noted that when T_M's are measured in an echo experiment with substantial dead time τ_d, then the long-time asymptotic features of the motions should be dominant, and this should mainly depend only on $R(0)$ which follows Brownian motional theory [i.e., the long-time behavior is dominated by the near-zero frequencies in the Fourier transform]. This will be true if the experimental time scale T_M ($\gtrsim \tau_d$) is of order of or greater than τ_M. The cw spectra, however, are not so coarse grained in time; i.e., they are sensitive to a wider range of frequencies (e.g., compare the small extent of the width axis in the 2*D* spectra of order T_2^{-1}, which is a measure of the near zero frequencies important in the observed echo decays vs the field axis multiplied by $\gamma_e/2\pi$).

While the effects of such a "fluctuating torque" model on the cw vs echo spectra requires further analysis for a proper understanding, it does relate, to some extent, to a significant difference between the two spectroscopies in how they reflect on motional dynamics. That is the cw spectra are determined by both the real parts of the Λ_j (i.e., the T_2's) as well as their imaginary parts which represent the frequency shifts and the latter are typically the more significant in determining the cw line shapes in the slow motional region. We may expect that these real and imaginary parts will reflect any memory effects in a somewhat different fashion (e.g., this was shown to be true for the spectral densities generated by the reorientations for such a model[7]).

Thus the cw spectra may be expected to be sensitive to the frequency dependence of $R(\omega)$ provided only that they are still in the model sensitive regime as was the case for the experiments of HMHF. The 2*D* ESE spectra sliced along the field axis are sensitive to the Im Λ_j in a way similar to the cw spectra. However, the Re Λ_j are highly resolved along the width axis. The potentially important role that cw-type spectra vs echo spectra could play in the study of molecular dynamics is seen from this illustration to be that the former largely reflect on the Im Λ_j while the latter reflect on the Re Λ_j. 2*D* echo spectroscopy, however, provides this complementary information along the two different frequency axes, but is at present limited in time resolution by the finite dead time.

We now wish briefly to consider the source of the dependence of the 2*D* contour patterns on model. This, we believe, is related to a discussion given by Schwartz *et al.*[1] for interpreting the different power law dependence of T_M on τ_R for the different models as found from theoretical simulations. Thus, they found $T_M \propto \tau_R^{1/2}$, $\tau_R^{2/3}$, and τ_R for the canonical models of Brownian, approximate free, and jump diffusion, respectively. The case of jump diffusion could be interpreted as leading to Heisenberg-uncertainty-in-lifetime broadening due to random rotational jumps at frequency τ_R^{-1}, which carries the molecule from one orientation to an arbitrarily different one. That is, for jumps of substantial rms angles, this effectively removes the molecule from one spectral region and brings it into another, in the near rigid limit. Since the jump rate in an isotropic fluid is independent of initial orientation, then the spin packets (corresponding roughly to molecules with the different initial orientations) will all be broadened by the same amount. Thus T_2 will be an invariant across the spectrum.

Brownian motion, wherein reorientational steps are infinitesimal in size, is better interpreted by another model. Kivelson and Lee[15] suggested that one interpret the T_2 from a molecule at a particular orientation in the near-rigid limit in a *restricted* motional narrowing sense. That is, one estimates the "motionally narrowed" T_2 resulting from reorientations within only the small range of angles that the molecule can sample in the time scale of the experiment, which is just of order T_2 itself. The fact that $T_2 \ll \tau_R$ guarantees that only a small range of angles is sampled (i.e., this is a nonergodic process). The value of T_2^{-1} for each orientation is then approximately determined in part by the quantity $\Delta\omega(\theta) \equiv [d\omega(\theta)/d\theta](\Delta\theta)$, which measures the amount of change of the near-rigid limit spectrum $\omega(\theta)$ for $\Delta\theta$, a small rotationally induced change in θ, the angle between the principal molecular magnetic tensor axis and the dc magnetic field. Thus, for example, for a simple rigid-limit ESR spectrum such that

$$\omega(\theta) = (A/2)(3\cos^2\theta - 1)$$

[e.g., if there were just an axially symmetric g tensor in $H_1(\Omega)$] then

$$\Delta\omega(\theta) \approx -\tfrac{3}{2}A[\Delta\theta^2 \cos 2\theta + \Delta\theta \sin 2\theta].$$

Then, for $\theta = 0°$ or $90°$, one has $\Delta\omega(\theta) \propto \Delta\theta^2$, or a higher order quantity, then for $\theta = 45°$ where $\Delta\omega(\theta) \propto \Delta\theta$. This means that spectral packets due to molecules with orientation $\theta \sim 45°$ will be more substantially broadened by the slow Brownian diffusion than those corresponding to the principal angles $\theta \sim 0°$ or $90°$. This trend is in accord with the variations in T_2, shown in Figs. 3, that were obtained from the

rigorous solutions to the SLE [Eq. (1)]. We have checked this point of view by simulating a 2*D* echo spectrum [using Eq. (1)] arising just from an axially symmetric *g* tensor for which the rigid-limit spectrum does, indeed, depend simply on $\frac{1}{2}(3\cos^2\theta - 1)$, and we found it to be consistent with the $\theta \sim 45°$ orientations yielding the shortest T_2's (i.e., broadest widths).

The approximate free diffusion model may be regarded as intermediate between the Brownian and jump models, so it would be expected to yield contours that are intermediate in appearance and this is so.

The reason why the predicted contours become parallel and model independent as $\tau_R \to \infty$ is not yet clear. It might be related to the fact that as $\tau_R \to \infty$, the physical character of the echo envelopes becomes different. In this limit they become dominated by an exponential decay in τ^3/τ_R which is found to be model *independent*,[1] rather than the exponential decay in τ/T_M which is model dependent. Of course, the *experimental* spectra, in the limit $\tau_R \to \infty$, will have their T_2's dominated by processes other than modulation of the spin Hamiltonian by the rotational reorientation.

V. SUMMARY AND PROSPECTUS

The two-dimensional electron spin echo (2*D*-ESE) technique described in this work has been shown to be applicable to the study of slow motions. It should have future applicability in the study of motional dynamics in viscous fluids by spin probe techniques and in the study of biological systems containing spin labels. The present spectral sensitivity is in the range of rotational correlation times τ_R of about 1–100 μs. The study reported herein has led to improved insights into the motional dynamics of the spin-probe Tempone in glycerol/H_2O solvent. A convenient theory for simulating the two-dimensional spectra in this range of τ_R was developed and employed to show the very significant sensitivity of the normalized 2*D* contours to the microscopic model of molecular reorientation. In particular, it was found that a Brownian model was the most satisfactory of the three canonical models considered for the experimental system studied.

The expression which describes this experiment [cf. Eq. (16)] shows that the normalized contour plots are actually a graph of the real vs the imaginary parts of the eigenvalues of the "dynamic spin packets." The real part determines the homogeneous T_2 due to the motion or alternatively the width of the spin packet, while the imaginary part gives its resonance frequency. However, while the T_2's may be obtained with inhomogeneous broadening absent, the resonant frequencies are convoluted with the inhomogeneous broadening. Thus 2*D* spectroscopy is clearly an advantage over conventional cw spectroscopy, wherein the spectrum is just constructed from an overlapping superposition of the spin packets, which usually provides poor resolution especially with regard to the motional T_2's (or widths) in the slow motional region.

Full realization of the potential of this 2*D* spectroscopy would, however, require significant reductions in dead time τ_d. This would enable the study of faster motions with improved signal to noise and would also lead to more definitive model dependences. One may expect that a variety of current techniques being developed in various laboratories will lead to significant reductions in τ_d. It should be remarked that the advantages of this 2*D* spectroscopy are the same as that of a conventional ESE experiment with the important differences that: (a) one maps in detail the T_2's across the whole spectrum, and also (b) various techniques of signal averaging and signal enhancement may be employed.

The basic 90°-τ-180°-τ pulse sequence used in this work is only one of several pulse sequences used in electron spin-echo studies.[16] For example, the stimulated echo sequence: 90°-τ-90°-T-90°-τ should be particularly useful as the basis of 2*D*-ESE spectroscopy for slow motional studies. It is used in ESE motional narrowing experiments as an alternative method to measure T_1 vs the conventional three-pulse sequence of 180°-T-90°-τ-180°-τ (wherein T is stepped in both experiments).[17] However, even in the motional narrowing regime these pulse sequences can be differently affected by nuclear-spin-flip and cross relaxation terms.[17] In the slow motional regime we find theoretically, and from preliminary experiments, that they yield significantly different results, with the T_1's from the stimulated echoes (i.e., T_1^{SE}) being much shorter.[18] Our theoretical analysis shows that the T_1 from the stimulated echo can be properly represented only by a sum of exponentials which depend upon the value of τ_R as well as the T_1. Thus, one may construct a two-dimensional ESE spectroscopy based upon this pulse sequence. Its advantage would be that, since $T_1 \gg T_2^{ss}$ in the slow motional region (where T_2^{ss} is the contribution to T_2 from solid-state processes),[8,13,18] then it would be possible to study much slower motions, limited only by $\tau_R \lesssim T_1$. In this connection, we note that Merks and de Beer[19] have used the stimulated echo sequence in a two-dimensional ESE experiment to facilitate spectral assignments in solids. We are currently working on such a technique for the study of slow motions.

Clearly, this example is one of a variety of possibilities for 2*D*-ESE (by analogy to 2*D*-NMR spectroscopy[3]). Another important technical development for ESE would be the ability to irradiate the whole spectrum with intense and short microwave pulses. Then the complete free-induction decays could be recorded to enable a two-dimensional experiment generated entirely in the time domain. This would have the advantages of (i) greatly reducing the data collection time, and (ii) permitting a more straightforward analysis than for field-swept pulsed experiments. Current efforts are under way in our laboratory toward this ambitious objective.

In conclusion, we believe that various forms of 2*D*-ESE spectroscopy will play an important role in the study of molecular motions in the future, and the potential has been hinted at by the present study.

ACKNOWLEDGMENTS

We wish to thank Mr. Dave Schneider for his extensive help with the computer graphics and Ms. Leslie Schwartz for many helpful discussions.

[1] L. J. Schwartz, A. E. Stillman, and J. H. Freed, J. Chem. Phys. 77, 5410 (1982).

[2]*Spin Labeling Theory and Applications*, edited by L. J. Berliner (Academic, New York, 1976).
[3]A. Bax, *Two-Dimensional Nuclear Magnetic Resonance in Liquids* (Delft University, Dordrecht, Holland, 1982).
[4]G. Moro and J. H. Freed, J. Phys. Chem. **84**, 2837 (1980); J. Chem. Phys. **74**, 3757 (1981).
[5]E. Bartholdi and R. R. Ernst, J. Magn. Reson. **11**, 9 (1972).
[6]T. Inouye, T. Harper, and N. C. Rasmussen, Nucl. Instrum. Methods **67**, 125 (1969). In this data smoothing study, windows with Gaussian tails were used; in our 2*D* experiments greater success (i.e., greater smoothing without significant signal distortion) was achieved with the sharper window generated from the function $\exp[-(t/a)^4]$.
[7]J. S. Hwang, R. P. Mason, L. P. Hwang, and J. H. Freed, J. Phys. Chem. **79**, 489 (1975).
[8]A. E. Stillman, L. J. Schwartz, and J. H. Freed, J. Chem. Phys. **73**, 3502 (1980).
[9](a) J. H. Freed, G. V. Bruno, and C. F. Polnaszek, J. Phys. Chem. **75**, 3385 (1971); (b) J. H. Freed, in *Spin Labeling Theory and Applications*, edited by L. J. Berliner (Academic, New York, 1976), Chap. 3.
[10]I. J. Lowe and R. E. Norberg, Phys. Rev. **107**, 46 (1957); R. R. Ernst, W. P. Aue, E. Bartholdi, A. Höhner, and S. Schämblein, Pure Appl. Chem. **37**, 47 (1974); R. R. Ernst and W. A. Anderson, Rev. Sci. Instrum. **37**, 93 (1966); D. Shaw, *Fourier Transform NMR Spectroscopy* (Elsevier, New York, 1976).
[11](a) A more reasonable form for our ESE experiment would be to replace the Lorentzians in Eq. (13) with width $T_{2,j}$ by a function of form $(\gamma H_1^2/\gamma H_1^2 + \Delta\omega_j'^2)^{n/2}$ $n \sim 2$ or 3 (where $\Delta\omega_j' = \omega' - \omega_j$) which is suggested by a rigid-limit echo result for spin packets. It is for the case of two equal pulses and is actually somewhat more complicated [cf. W. B. Mims, Rev. Sci. Instrum. **36**, 1472 (1965)]. The main point is that for $|\gamma H_1| \ll \Delta$ we again obtain Eq. (15); (b) If there were no inhomogeneous broadening, then Eq. (12) would still not be appropriate for our experiment even in the lim $\gamma H_1 \ll T_{2,j}^{-1}$. The effect of such a small H_1 in rotating a spin packet, in this limit, is more complicated but could be analyzed in detail by the formalism developed previously for time-domain ESR experiments under the condition that $|\gamma H_1|/|T_{2,j}^{-1} + i(\omega' - \omega_j)| \ll 1$ [cf. J. H. Freed, J. Phys. Chem. **78**, 1155 (1974)] and in *Time Domain Electron Spin Resonance*, edited by L. Kevan and R. N. Schwartz (Plenum, New York, 1979), Chap. 2. Of course, in this limit there is a tremendous loss in signal to noise, rendering such an experiment impractical for slow-motional spectra.
[12]D. Kivelson and P. A. Madden, Annu. Rev. Phys. Chem. **31**, 523 (1980).
[13]J. P. Hornak and J. H. Freed, Chem. Phys. Lett. **101**, 115 (1983); in this echo-ELDOR study a *preliminary* analysis based on the strong-jump limiting model yielded τ_R's of the order obtained in the present work with the model of approximate free diffusion for those temperatures which overlapped with this study.
[14]A more recent discussion of experimental evidence for such a "fluctuating torque model" as well as a related slowly relaxing local structure model for Tempone may be found in S. A. Zager and J. H. Freed, J. Chem. Phys. **77**, 3344, 3360 (1982).
[15]D. Kivelson and S. Lee, J. Chem. Phys. **76**, 5746 (1982).
[16]*Time-Domain Electron Spin Resonance*, edited by L. Kevan and R. N. Schwartz (Wiley, New York, 1979).
[17]A. E. Stillman and R. N. Schwartz, J. Phys. Chem. **85**, 3031 (1981).
[18]L. J. Schwartz, G. L. Millhauser, and J. H. Freed (unpublished).
[19]R. P. J. Merks and R. de Beer, J. Phys. Chem. **83**, 3319 (1979).